

Article

Comparative Analysis of Binding Kinetics and Thermodynamics of Dipeptidyl Peptidase-4 Inhibitors and Their Relationship to Structure

Gisela Schnapp, Thomas Klein, Yvette Hoevels, Remko A. Bakker, and Herbert Nar

J. Med. Chem., **Just Accepted Manuscript** • DOI: 10.1021/acs.jmedchem.6b00475 • Publication Date (Web): 20 Jul 2016

Downloaded from <http://pubs.acs.org> on July 26, 2016

Just Accepted

“Just Accepted” manuscripts have been peer-reviewed and accepted for publication. They are posted online prior to technical editing, formatting for publication and author proofing. The American Chemical Society provides “Just Accepted” as a free service to the research community to expedite the dissemination of scientific material as soon as possible after acceptance. “Just Accepted” manuscripts appear in full in PDF format accompanied by an HTML abstract. “Just Accepted” manuscripts have been fully peer reviewed, but should not be considered the official version of record. They are accessible to all readers and citable by the Digital Object Identifier (DOI®). “Just Accepted” is an optional service offered to authors. Therefore, the “Just Accepted” Web site may not include all articles that will be published in the journal. After a manuscript is technically edited and formatted, it will be removed from the “Just Accepted” Web site and published as an ASAP article. Note that technical editing may introduce minor changes to the manuscript text and/or graphics which could affect content, and all legal disclaimers and ethical guidelines that apply to the journal pertain. ACS cannot be held responsible for errors or consequences arising from the use of information contained in these “Just Accepted” manuscripts.

1
2
3 **Comparative Analysis of Binding Kinetics and Thermodynamics of Dipeptidyl Peptidase-**
4 **4 Inhibitors and Their Relationship to Structure**
5
6
7

8
9
10 Gisela Schnapp, Thomas Klein, Yvette Hoevels, Remko A. Bakker, and Herbert Nar*
11

12
13
14 Department of Lead Identification and Optimization Support and Department of CardioMetabolic
15 Diseases Research, Boehringer Ingelheim Pharma GmbH & Co. KG, Biberach, Germany
16
17
18

19
20
21 **Address for correspondence:**
22

23 *Dr Herbert Nar
24

25 Department of Lead Identification and Optimization Support,
26

27 Boehringer Ingelheim Pharma GmbH & Co. KG,
28

29 Birkendorferstr. 65,
30

31 88397 Biberach,
32

33 Germany
34
35
36
37
38
39
40
41
42
43
44
45
46
47
48
49
50
51
52
53
54
55
56
57
58
59
60

1
2
3 **ABSTRACT:** The binding kinetics and thermodynamics of dipeptidyl peptidase (DPP)-4
4 inhibitors (gliptins) were investigated using surface plasmon resonance and isothermal titration
5 calorimetry. Binding of gliptins to DPP-4 is a rapid electrostatically driven process. Off-rates
6 were generally slow partly because of reversible covalent bond formation by some gliptins, and
7 partly because of strong and extensive interactions. Binding of all gliptins is enthalpy-dominated
8 due to strong ionic interactions and strong solvent-shielded hydrogen bonds. Using a
9 congeneric series of molecules which represented the intermediates in the lead optimization
10 program of linagliptin, the onset of slow binding kinetics and development of the thermodynamic
11 repertoire were analyzed in the context of incremental changes of the chemical structures. All
12 compounds rapidly associated and therefore the optimization of affinity and residence time are
13 highly correlated. The major contributor to the increasing free energy of binding was a strong
14 increase of binding enthalpy, whereas entropic contributions remained low and constant despite
15 significant addition of lipophilicity.
16
17
18
19
20
21
22
23
24
25
26
27
28
29
30
31
32
33
34
35
36
37
38
39
40
41
42
43
44
45
46
47
48
49
50
51
52
53
54
55
56
57
58
59
60

INTRODUCTION

Dipeptidyl peptidase-4 (DPP)-4 is a widely distributed, membrane-bound, but also secreted, serine protease. It is responsible for the rapid inactivation of the incretin hormones glucagon-like peptide (GLP)-1 and glucose-dependent insulinotropic peptide (GIP) via cleavage of a dipeptide from the N-terminus of these oligopeptides.¹ GLP-1 and GIP are released from the gut in response to food intake and exert a potent glucose-dependent insulinotropic action, thereby contributing to the maintenance of postprandial glycemic control.² GLP-1 is also involved in the inhibition of postprandial glucagon secretion from pancreatic α -cells, retardation of gastric emptying, suppression of appetite leading to reduction in food intake, and direct beneficial effects on pancreatic β -cells.^{3,4} Inhibition of DPP-4 prolongs the residence time and consequently the activity of GLP-1 and GIP. Inhibition of GLP-1 and GIP metabolic breakdown improves glycemic control in patients with type 2 diabetes, making DPP-4 a good therapeutic target.⁵

Dipeptidyl Peptidase-4. DPP-4 is a serine exo-dipeptidase and a member of the prolyl oligopeptidase family. It is highly specific in recognizing peptide substrates with proline or alanine in the last position (P1) prior to the scissile amide bond. DPP-4 exists as a homodimer consisting of 766 amino acids with cytoplasmic, transmembrane, and extracellular regions. The extracellular part is divided into a β -propeller domain and a catalytic $\alpha\beta$ -hydrolase domain with the catalytic triad Ser630–Asp708–His740.⁶ The active site of the DPP-4 enzyme lies within a large cavity formed by these domains and includes the catalytic Ser630 and the oxyanion hole (Tyr631, Tyr547), a hydrophobic S1 pocket (Tyr631, Val656, Trp659, Tyr662, Tyr666, and Val711), and an S2 pocket. Substrates can access the active site through a tunnel in the β -propeller or via a side opening.

1
2
3 **Approved DPP-4 Inhibitors.** Several DPP-4 inhibitors (gliptins) have been successfully
4 launched and have shown clinically good efficacy and safety in patients with type 2 diabetes.
5
6 The currently worldwide marketed DPP-4 inhibitors sitagliptin, vildagliptin, saxagliptin, linagliptin,
7
8 alogliptin, and teneligliptin (tenegliptin launched in Japan and Argentina) have distinct chemical
9
10 structures which confer different potency and selectivity profiles, as well as pharmacokinetic and
11
12 pharmacologic properties, and display different modes of binding.⁷⁻⁹ Vildagliptin and saxagliptin
13
14 are peptide mimetic compounds, which were discovered by building on the substrate-derived
15
16 Gly–Pro dipeptide scaffold. Teneligliptin was developed from a prolylthiazolidine core as a
17
18 proline mimetic.¹⁰ In contrast, sitagliptin, alogliptin, and linagliptin were discovered by screening
19
20 and lead optimization (LO).
21
22
23
24
25
26

27 **Structural Information on Gliptin Binding to DPP-4.** X-ray co-crystal structures of all
28
29 gliptins are reported (see Yoshida et al,¹⁰ Eckhardt et al,¹¹ and Nabeno et al,⁹ and references
30
31 therein). Although the chemical structures are different, all DPP-4 inhibitors are substrate-
32
33 competitive active site binders and have common interactions with key residues of the target
34
35 protein. Primary or secondary amino groups interact with the recognition site for the peptide
36
37 substrate N-terminus (Glu205, Glu206, and Tyr662, the “amino hot-spot”) of DPP-4 via the
38
39 formation of two or three charge-reinforced hydrogen bonds. The hydrophobic S1 pocket of
40
41 DPP-4 is occupied by hydrophobic inhibitor moieties, while the S2 pocket is filled by other
42
43 substituents.
44
45

46 Vildagliptin and saxagliptin are cyanopyrrolidine inhibitors and form a covalent but
47
48 reversible complex with DPP-4 through the formation of an imino ester with the hydroxyl group
49
50 of the catalytic serine S630. Both inhibitors have a bulky adamantyl group which occupies the
51
52 S2 pocket in a similar position, but with the hydroxyl group in different orientations (Figure 1a).
53
54 Both vildagliptin and saxagliptin bind to the target without inducing any conformational change
55
56 to the protein. Teneligliptin and sitagliptin occupy the active site in a linear conformation (Figure
57
58
59
60

1
2
3 1b). Their binding leads to a conformational change involving Arg358, which adopts a distinct
4 side-chain reorientation that facilitates the opening of a hydrophobic pocket termed the
5 extended S2 pocket. The phenyl and trifluoromethyl moieties of sitagliptin and teneligliptin,
6
7 extended S2 pocket. The phenyl and trifluoromethyl moieties of sitagliptin and teneligliptin,
8
9 respectively, occupy this induced pocket. The binding of linagliptin and alogliptin to DPP-4 is
10
11 accompanied by a different conformational change involving Tyr547, which allows the formation
12
13 of a π -stacking interaction with the xanthine and uracil cores of linagliptin and alogliptin,
14
15 respectively. Both inhibitors form an H-bond with the backbone NH of Tyr631 utilizing a carbonyl
16
17 oxygen H-bond acceptor group in their heterocyclic cores. The binding of linagliptin to DPP-4
18
19 involves extensive hydrophobic interactions of its 1-quinazoline substituent within the S1'-S2'
20
21 pockets, mainly with the Trp629 indole side-chain (Figure 1c). It should be noted that the crystal
22
23 structures that will be used below to discuss structure-biophysics relationships were derived
24
25 from two orthologs of DPP-4 (porcine for linagliptin precursors **1** and **2** and human for all
26
27 others), from distinct crystal forms and co-crystals were obtained under different conditions.
28
29 However, as discussed above, the ligand binding site of DPP-4 is in a large cavity and,
30
31 therefore, distinct crystal packing will probably not affect the ligand binding mode and interaction
32
33 patterns.
34
35
36
37
38
39

40 **Binding Kinetics and Thermodynamics in Drug Discovery.** During the drug
41
42 discovery process, there is considerable interest in the key parameters of binding kinetics and
43
44 thermodynamics for compound selection and optimization.¹²⁻¹⁶ For instance, drugs with
45
46 prolonged off-rates may be attractive from a pharmacologic perspective because once bound to
47
48 the target, they can potentially inhibit the enzyme function even after the free drug has been
49
50 cleared from circulation. This rare situation occurs if the binding kinetics of the drug are much
51
52 slower than its pharmacokinetics.
53
54

55 It is discussed widely in the literature that selection of compounds with a strong
56
57 contribution of enthalpy to the free energy of binding is advised in the early phases of a drug
58
59
60

1
2
3 discovery process, because chemical optimization often involves the addition of hydrophobic
4 groups which mainly impact binding entropy. Binding enthalpy, in contrast, is more difficult to
5 optimize.^{15, 17} Although increasing numbers of publications describe experimental data, the
6 molecular determinants of binding kinetic and thermodynamic profiles are still only scarcely
7 understood, and comprehensive information on the development of these parameters in a
8 congeneric series of compounds remains rare.

9
10
11
12
13
14
15
16 DPP-4 inhibitors are known to have relatively long residence times on their target
17 protein.^{7, 18, 19} However, no comparative studies of biophysically derived binding kinetics for the
18 approved DPP-4 inhibitors have been reported to date. In the present study, we investigated the
19 binding kinetics and thermodynamics of DPP-4 inhibitors using surface plasmon resonance
20 (SPR) and isothermal titration calorimetry (ITC) studies. In addition, a retrospective biophysical
21 study was conducted on a series of congeneric compounds representing key intermediates in
22 the drug discovery process leading to linagliptin. Results will be discussed regarding the binding
23 modes of these compounds to the DPP-4 active site, and some conclusions made concerning
24 emerging structure–kinetic and structure–thermodynamic relationships.

25 26 27 28 29 30 31 32 33 34 35 36 37 38 **RESULTS AND DISCUSSION**

39 40 41 42 **Gliptins are Low Nanomolar or Sub-nanomolar Inhibitors of Human DPP-4.**

43
44
45
46
47
48
49
50
51
52
53
54
55
56
57
58
59
60
Linagliptin was the most potent inhibitor of DPP-4 activity using human recombinant enzyme or
enzyme derived from human plasma. The IC_{50} was 1.4 nM (Supplementary Table S1), which is
consistent with data previously published by Thomas et al using human Caco-2 cell extracts.²⁰
With an enzyme concentration of approximately 1 nM in both assays, the activity of linagliptin is
most probably beyond the detection limit (assay wall) so that its IC_{50} reflects an upper limit to its
real potency.

1
2
3 The other DPP-4 inhibitors showed lower potencies, ranging from 7 nM for alogliptin to
4
5 95 nM for vildagliptin (Supplementary Table S1). Teneeligliptin was the only DPP-4 inhibitor that
6
7 showed a weaker affinity for the enzyme derived from human plasma than for the human
8
9 recombinant enzyme. However, the numerical differences were relatively small and may lie
10
11 within the analytical variability of the assay.
12
13

14
15
16 **DPP-4 Inhibitors Associate Rapidly With Their Target.** SPR sensorgrams describing
17
18 the binding kinetics of each DPP-4 inhibitor are shown in Figure 2. Quantitative data analysis
19
20 indicated that linagliptin is a low picomolar binder with the highest affinity for DPP-4, followed by
21
22 saxagliptin and teneeligliptin which exhibited binding affinities of 0.3 nM and 0.4 nM, respectively.
23
24 Sitagliptin, alogliptin, and vildagliptin were significantly less potent with low single-digit
25
26 nanomolar binding affinities.
27
28

29 The on-rates of all DPP-4 inhibitors were generally fast and within the range of 10^5 – 10^7
30
31 $M^{-1}s^{-1}$. On-rates of the primary amines (alogliptin, sitagliptin, and linagliptin) were close to the
32
33 diffusion limit ($>10^6 M^{-1}s^{-1}$), whereas the secondary amines (vildagliptin, saxagliptin, and
34
35 teneeligliptin) were associated with at least 10-fold slower on-rates (approximately $10^5 M^{-1}s^{-1}$).
36
37 For example, for the two structurally similar reversible covalent inhibitors vildagliptin and
38
39 saxagliptin, the on-rate of the secondary amine vildagliptin was $7.1 \times 10^4 M^{-1}s^{-1}$, whereas the
40
41 primary amine saxagliptin showed a faster on-rate of $9.2 \times 10^5 M^{-1}s^{-1}$.
42
43
44

45 There is ample evidence in the current literature, summarized in a review by Pan et al
46
47 2013²¹, which shows that electrostatic interactions between a charged drug and a reversely
48
49 charged protein positively impact association rates. Based on this evidence, we assumed that
50
51 binding of gliptins to DPP-4 is a rapid electrostatically driven process with a dominant influence
52
53 of attractive Coulomb forces on the association rates. The localized positive charge on the
54
55 ligand is sensed by the negatively charged surface patch at the Glu205/6 dyad in the DPP-4
56
57 active site leading to an acceleration of the bimolecular binding process. Because the charge
58
59
60

1
2
3 density on the ammonium functions is higher for primary than secondary amines, the former
4 exhibit a faster association rate than the latter.
5
6
7

8 9 **Structurally Distinct DPP-4 Inhibitors Exhibit Distinct Target Dissociation**

10 **Behavior.** Sitagliptin and alogliptin had relatively fast off-rates of 0.063 s^{-1} and 0.0031 s^{-1} ,
11 respectively. The covalent binders vildagliptin and saxagliptin had much slower dissociation
12 rates of $1.7 \times 10^{-4} \text{ s}^{-1}$ and $2.0 \times 10^{-4} \text{ s}^{-1}$, respectively. The off-rate of teneligliptin was slow ($2.6 \times$
13 10^{-4} s^{-1}) and similar to the covalent binders. Linagliptin had the slowest dissociation rate ($5.1 \times$
14 10^{-5} s^{-1}), corresponding to a residence time of 327min (Figure 2).
15
16
17
18
19
20
21

22 For the slowly dissociating compounds, SPR experiments had to be performed in a
23 single-cycle kinetics setting, and dissociation times needed to be sufficiently long to observe a
24 significant decline in the sensorgrams. This was especially the case for linagliptin, where values
25 were at the detection limit of the instrumentation. Validation of the SPR-derived dissociation
26 rates was therefore sought through comparisons with other kinetic data for gliptins from the
27 literature. There are two reports on DPP-4 inhibitor binding kinetics based on enzyme kinetics
28 for four of the six compounds under investigation. The k_{off} values determined using SPR are in
29 good agreement with off-rates obtained by enzyme activity recovery assays reported by Thomas
30 et al (linagliptin $3.0 \times 10^{-5} \text{ s}^{-1}$; vildagliptin $2.1 \times 10^{-4} \text{ s}^{-1}$),²⁰ and Wang et al (saxagliptin 2.3×10^{-4}
31 s^{-1} ; sitagliptin $>5.8 \times 10^{-3} \text{ s}^{-1}$).²²
32
33
34
35
36
37
38
39
40
41
42
43
44
45

46 **Structure–Kinetic Relationships.** The dissociation rates of the gliptins range from a
47 relatively fast off-rate regime (sitagliptin and alogliptin with residence times of 0.26 min and 5.4
48 min, respectively) to a slow off-rate regime (327 min for linagliptin). This slow dissociation
49 behavior can be attributed to either reversible covalent bond formation (saxagliptin and
50 vildagliptin), or to strong and extensive interactions that both pose a large energy barrier for
51 dissociation (teneligliptin and linagliptin).
52
53
54
55
56
57
58
59
60

1
2
3 The reversible covalent binders vildagliptin and saxagliptin show very similar interactions
4
5 in their active sites and do not induce any conformational change in the protein. Both inhibitors
6
7 have nanomolar affinities and prolonged off-rates resulting in residence times of the
8
9 corresponding enzyme complexes of approximately 1.5 hours. We assumed that the slow
10
11 dissociation kinetics is a result of the increased activation barrier posed by the cleavage of the
12
13 imino ester bonds involving S630. Although the associated reaction kinetics for the ester bond
14
15 cleavage is fast, it is the stability of the covalent complexes that leads to a substantial
16
17 contribution to off-rate prolongation. Saxagliptin, which is a close analog lacking the cyano
18
19 warhead, exhibits a 20-fold lower K_i .²³ Assuming similar on-rates for the pair of compounds, the
20
21 analog should dissociate 20-fold faster than saxagliptin, yielding a compound with fast binding
22
23 kinetics.
24
25

26
27 The essential structural elements for the long residence times of teneligliptin and
28
29 linagliptin presumably are moieties that either form enhanced hydrogen-bonding interactions or
30
31 cover larger hydrophobic surface areas. This assumption is supported by literature reports
32
33 suggesting a prominent role of hydrogen bonds that are shielded from water by surrounding
34
35 hydrophobic regions in the optimization of residence times.²⁴ For example, comparing linagliptin
36
37 and alogliptin, the 1-quinazoline group of linagliptin covers a large hydrophobic surface patch in
38
39 the S1'–S2' region of the DPP-4 active site, mainly with the Trp629 indole side-chain, and
40
41 simultaneously shields the hydrogen bond of its core carbonyl oxygen to the backbone NH of
42
43 Tyr631. The analogous hydrogen bond of alogliptin is hydrophobically shielded to a lesser
44
45 extent because of the absence of a hydrophobic substituent in an analogous position. As a
46
47 result, the hydrogen bond is more exposed to solvent and more easily replaced by water.
48
49 Therefore, significantly higher binding affinity and slower dissociation of linagliptin compared
50
51 with alogliptin may in part be explained by an efficient solvent-shielding effect of this crucial
52
53 hydrogen bond.
54
55
56
57
58
59
60

1
2
3 Conformational changes are a prominent feature of many protein–ligand interactions
4 with slow dissociation kinetics.^{12, 25} Binding of some gliptins is associated with a change in the
5 conformation of the DPP-4 active site, mainly because of side-chain rotations about Arg358
6 (sitagliptin and teneligliptin) or Tyr547 (linagliptin and alogliptin).
7
8
9

10 Surprisingly, in the present study, pairs of DPP-4 inhibitors which have similar binding to
11 the active site of DPP-4 show dissimilar binding kinetics (Supplementary Figure S1).
12
13 Teneligliptin and sitagliptin induce the same conformational change involving Arg358, and in a
14 similar way occupy the induced hydrophobic extended S2 pocket with their phenyl and
15 trifluoromethyl moieties. However, these common hydrophobic interactions in the extended S2
16 pocket as well as the necessary conformational changes seem to have no dominant role in
17 binding kinetics, because sitagliptin has a much faster off-rate than teneligliptin.
18
19
20
21
22
23
24
25
26

27 The binding of linagliptin and alogliptin to DPP-4 is accompanied by a different
28 conformational change involving Tyr547, which allows the formation of a π -stacking interaction
29 with the xanthine core of linagliptin. Again, this conformational change has no dominant role in
30 determining binding kinetics because both inhibitors differ in their off-rates by two orders of
31 magnitude.
32
33
34
35
36
37
38
39

40 **Gliptins are Enthalpic DPP-4 Binders.** ITC measures the binding enthalpy by detecting
41 the heat absorbed or released during a bimolecular binding event. One limitation of ITC is its
42 application to compounds with extraordinarily high potency, such as some of the DPP-4
43 inhibitors used in this study. The calculation of the association constant K_a from the slope of the
44 binding isotherm in such a case is problematic owing to its steepness. The most potent DPP-4
45 inhibitor, linagliptin, showed the steepest binding isotherm, requiring therefore that the K_D value
46 for linagliptin be determined using a complementary competition experiment. Use of the
47 competitor led to the expected significantly lower K_D value and to minor changes in the
48 thermodynamic signature of linagliptin (Supplementary Figure S2). For the other DPP-4
49
50
51
52
53
54
55
56
57
58
59
60

1
2
3 inhibitors, the binding isotherms were well fitted (Supplementary Figure S3). Therefore,
4
5 determination of the entropic and enthalpic contributions was possible and comparisons made
6
7 using the derived data. For consistency, the thermodynamic signature of linagliptin from direct
8
9 ITC in the absence of a competitor ligand was used to compare it with the other gliptins. Binding
10
11 of all DPP-4 inhibitors was driven by strong enthalpic contributions. Relatively minor entropic
12
13 contributions were observed (Figure 3).
14

15
16 The partially solvent-shielded charge-reinforced hydrogen bonds formed between the
17
18 cationic primary and secondary amines of the inhibitors and the active site amino hot-spot
19
20 pharmacophore, representing the major interaction formed by all DPP-4 inhibitors, may be the
21
22 major component of the strong enthalpic contribution.
23

24
25 Alogliptin and linagliptin have comparable thermodynamic signatures that correspond to
26
27 their similar binding interactions. However, despite a similar binding mode and inhibition
28
29 mechanism, vildagliptin and saxagliptin displayed significantly different binding thermodynamics.
30
31 Binding of vildagliptin exhibited a substantial entropic penalty, which was compensated for by a
32
33 much larger enthalpic contribution to binding, resulting in similar free energies of binding for the
34
35 two covalent inhibitors. This finding is difficult to interpret using existing structural information. A
36
37 plausible explanation for this phenomenon may be that the orientation of the hydroxyadamantyl
38
39 group is inverted between the two complex structures, despite identical substructures and
40
41 similar intermolecular interactions. The different ligand orientations will have a significant effect
42
43 on the surrounding water structure which was shown previously to have a major impact on the
44
45 partitioning of free energy.^{17, 26, 27}
46
47

48
49 Both teneligliptin and sitagliptin had favorable entropic contributions to the binding
50
51 energy that could result from desolvation because of hydrophobic interactions in the extended
52
53 S2 pocket. In contrast to sitagliptin, teneligliptin has a secondary amine which can form only two
54
55 hydrogen bonds with the amino hot-spot. This may be the reason for diminished binding
56
57 enthalpy.
58
59
60

1
2
3 In recent years, detailed analyses of binding thermodynamics for a number of model
4 systems have been published, including the interpretation of the dominating role of the water
5 structure using high resolution crystallographic structural information ($<1.5 \text{ \AA}$).¹⁷ Protein–ligand
6 co-structures with very high resolution and quality are required to allow complete modeling of
7 the solvent structure around the binding site and its comparison with the solvent structure in the
8 non-liganded protein. For the gliptins, structures were determined at 2.1–2.6 Å resolution.
9 Inspection of the structural models and the corresponding electron densities showed that
10 despite almost equivalent reported resolution, the quality of the experimental data, manifested in
11 the electron densities, as well as the extent to which the data were used to model the water
12 structure, deviate significantly. Consequently, a comparative interpretation of the role of the
13 water structure for the gliptins is precluded. For instance, although the two covalently bound
14 gliptins saxagliptin (3BJM) and vildagliptin (3W2T) were determined at practically identical
15 resolutions (2.35 Å), the elaboration of the solvent structure is dramatically different (with 2/3
16 versus 13/13 modelled water molecules in the two protomers in the asymmetric unit). For
17 saxagliptin, more water molecules could actually be built into the model based on an analysis of
18 the difference electron density. Future work on this aspect could utilize *in silico* approaches
19 such as WaterMap^{28, 29} or GIST^{30, 31} to obtain estimates of solvent energies using explicit solvent
20 modeling in addition to the crystallographic information.
21
22
23
24
25
26
27
28
29
30
31
32
33
34
35
36
37
38
39
40
41
42
43

44 **Comparison of Quantitative Binding and Potency Data, and Validity of Biophysical**
45 **Data.** In the above, quantitative binding and activity data for the family of DPP-4 inhibitors have
46 been presented. A direct comparison of the data showed that the calculated binding affinities
47 (K_D) from SPR data are numerically lower than those determined using a biochemical assay or
48 ITC. A plausible explanation for this difference is that for the enzymatic activity data, a lower
49 limit to the IC_{50} is set by the assay wall which is in the 1 nM range in the current experimental
50 setting, whereas the higher sensitivity SPR method is not limited by any assay wall.
51
52
53
54
55
56
57
58
59
60

1
2
3 In ITC, as described above, the high potency of the compounds and the corresponding
4 steepness of the binding isotherms may result in a systematic overestimation of the K_D . In such
5 a scenario, application of competition ITC is indicated to derive more reliable K_D values.
6
7

8
9 However, the addition of a competing ligand may also affect the thermodynamic signature.³²
10

11
12 The K_D calculations from SPR experiments could be influenced by a mass transport
13 limitation.³³ Moreover, the curve fitting in SPR for very slow off-rates (e.g., for linagliptin) is at
14 the limit of the instrument's specification. The long wash-out times required for a significant level
15 of dissociation may be confounded by target dissociation from the sensor surface, and
16 therefore, could cause uncertainty in the calculation of the K_D value. However, the off-rates
17 obtained by SPR are in good agreement with values obtained by enzymatic activity recovery
18 assays.
19
20
21
22
23
24
25
26

27 In all assays, linagliptin consistently had, by far, the highest affinity and the longest
28 residence time among DPP-4 inhibitors.
29
30
31
32

33 **Biophysical Analysis of a Congeneric Series of Linagliptin Precursors.** In the early
34 phases of an LO program in medicinal chemistry, optimization of a given lead candidate
35 traditionally involves improving its binding affinity. In contrast, recent discussions in the field
36 have focused on the importance of using binding kinetics, especially the dissociation rate, as the
37 primary optimization parameter and binding thermodynamics as a key element of lead
38 selection.^{15, 34-37}
39
40
41
42
43
44
45

46 Here, the current retrospective analysis has reviewed a congeneric series of DPP-4
47 inhibitors. SPR and ITC were used to determine how the kinetic and thermodynamic signatures
48 of the binding event developed during the optimization process, leading to the development of
49 linagliptin.
50
51
52
53
54

55 Xanthine derivative **1** was discovered using a high-throughput screening (HTS) process
56 and showed promising inhibitory activity in the low micromolar range (Figure 4a). The focus of
57
58
59
60

1
2
3 the LO program was on the variation of substituents at positions 1, 3, 7, and 8 of the xanthine
4 core. In the initial phases, a 50-fold increase in potency was achieved by replacing the 8-
5 piperazine moiety with a 3-amino piperidine (Figure 4b). Further variations at position 1, made
6 by attaching hydrophobic/aromatic substituents like benzyl, phenethyl, or phenacetyl, increased
7 the potency by a factor of 15. Compound **3** (Figure 4c) was the first long-acting inhibitor in the
8 lead series with an IC_{50} of 5 nM. However, this compound showed unacceptably high inhibition
9 of hERG channels ($IC_{50} = 200$ nM) and a high affinity for muscarinic receptors M1 (50 nM), M2,
10 and M3 (both ~ 150 nM). Therefore, further optimization of substituents at positions 7 and 1
11 focused on improving the specificity profile to avoid these off-target effects. Linagliptin finally
12 demonstrated extraordinarily high potency against DPP-4 and a clean off-target profile.^{11, 20} Only
13 the M1 receptor was inhibited at an IC_{50} of 300 nM, which is clinically irrelevant because of the
14 low C_{max} value of 10 nM in plasma resulting from the 5-mg dose of linagliptin used in clinical
15 practice.

16
17
18 In the SPR analysis, the initial HTS hit **1** showed transient binding kinetics, with a K_D
19 value of 806 nM determined from affinity plots (Figure 5). Substitution at position 8 increased
20 the potency ($K_D = 13.2$ nM) and led to a quantifiable binding kinetic profile for compound **2** ($k_{off} =$
21 0.064 s⁻¹). Compound **3** is a high affinity inhibitor (0.42 nM) with a slow off-rate of 0.00186 s⁻¹
22 and a residence time of 8.9 min. Finally, a further substantial increase in affinity for linagliptin is
23 based on the considerable increased residence time of the DPP-4 complex (327 min).

24
25
26 On examination of the congeneric series of ligands by ITC, binding was found to be
27 driven mainly by enthalpy. Compound affinity optimization was accompanied by increasing
28 binding enthalpy (Figure 6 and Supplementary Figure S4). The entropic contributions within this
29 lead series were negligible. The initial xanthine derivative **1** had a minor favorable entropic
30 contribution to the binding that was lost in compounds **2** and **3**. In contrast, linagliptin had a
31 small unfavorable contribution of binding entropy.

1
2
3 The series of linagliptin and its precursors bind to the active site in a conserved binding
4 mode (Figure 7). Binding of all compounds involves a conformational change of the Tyr547
5 side-chain. This facilitates formation of a π -stacking interaction of the phenol moiety of Tyr547
6 and the xanthine core of the inhibitors. Further, the xanthine core forms a hydrogen bond with
7 the C-6 carbonyl function of the xanthine scaffold to the backbone NH of Tyr631, which is
8 another conserved interaction within the compound series. Occupation of the S1 pocket is
9 facilitated by different hydrophobic substituents at position 7 of the xanthine core. The cationic
10 amino functionality interacting with the amino hot-spot of the active site changes from a
11 secondary amine in compound **1** to a tertiary amine in compounds **2**, **3**, and linagliptin. The
12 introduction of the amino-piperidine moiety in place of the piperazine ring has a strong impact
13 on potency, mainly because its primary amino group is sterically better positioned to interact
14 with the amino hot-spot of the target active site where it can form three instead of two hydrogen
15 bonds, leading to tighter interactions compared with the secondary amine of the initial HTS hit **1**.
16 Finally, a more lipophilic moiety of the xanthine core is present in compound **3** and linagliptin,
17 which leads to burial of a larger area of hydrophobic surface on the receptor by a π -stacking
18 interaction of the quinazoline moiety with Trp629, and to an increased shielding from water of
19 the hydrogen bond between the xanthine and the NH group of Tyr631. No considerable
20 rearrangement of the protein structure was observed between the different ligand complexes
21 which would produce major differences in thermodynamic signatures.

22
23
24
25
26
27
28
29
30
31
32
33
34
35
36
37
38
39
40
41
42
43
44
45
46
47
48
49
50
51
52
53
54
55
56
57
58
59
60

On the basis of this structural information, we conclude that the essential structural elements for off-rate improvement are the moieties that either form enhanced hydrogen bonding interactions or cover larger hydrophobic surface areas like the quinazoline group.

The on-rate in this series lies between 10^6 and $10^7 \text{ M}^{-1} \text{ s}^{-1}$ for all compounds and was largely unaffected during the optimization process. As mentioned above for the gliptins, it is presumed that the association process for these compounds is electrostatically dominated leading to fast on-rates close to the diffusion limit. As a consequence, during the optimization

1
2
3 process aimed at improving affinity, the increase in residence time (decrease in k_{off}) largely
4
5 develops in parallel with the binding affinity. In the case of LO of DPP-4 inhibitors, therefore,
6
7 focusing on either affinity or residence time as primary optimization parameters would most
8
9 probably not have affected the course of the project.
10

11
12 The original HTS compound **1** is a DPP-4 ligand with a dominant enthalpic contribution
13
14 to the free energy of binding. The optimization process and the gain in the free energy of
15
16 binding is mainly because of an increase in the enthalpic component, entropic contributions
17
18 playing a minor role in the compound's thermodynamic repertoire. Only linagliptin has a small
19
20 unfavorable contribution of binding entropy that may result from entropy–enthalpy compensation
21
22 for this high affinity compound.
23

24
25 All compounds in the congeneric series exhibit relatively low logD values (in the range of
26
27 0.0 to 1.6) and are thus relatively hydrophilic compounds. However, despite significant addition
28
29 of lipophilicity during the optimization process (Supplementary Figure S5), the entropic
30
31 contributions were not affected; however, enthalpic contributions were increased. This trend
32
33 was initially unexpected because the obvious consequence of utilizing the hydrophobic effect for
34
35 improving the free energy of binding by burial of the hydrophobic surfaces and release of
36
37 surface bound water molecules would be an increase in the entropic signature. Instead, the fact
38
39 that the enthalpic contribution was enhanced by these additional lipophilic interactions may be
40
41 interpreted by both displacement by the ligand of water molecules with high residual mobility
42
43 and an improvement of the water network established on the surface of newly formed
44
45 complexes. Examples of this behavior have been described previously.^{17, 26, 38, 39}
46
47

48
49 On interpretation of these data, it should be noted that changes in the individual
50
51 solvation pattern resulting from differences of just one single water molecule can strongly
52
53 perturb and shift the thermodynamic signatures between ligands.^{17, 26, 27} In the given series of
54
55 compounds, the structural information shows distinct water networks which explains why the
56
57
58
59
60

1
2
3 thermodynamic profiles cannot be fully interpreted by differences in lipophilicity or interaction
4
5 patterns alone.
6

7
8 Finally, within the series of congeneric compounds generated in the LO program for
9
10 linagliptin, a dependency was found between k_{off} values and the binding affinity/binding
11
12 enthalpy. This is in line with earlier observations suggesting that longer residence times are a
13
14 direct consequence of enhancing the enthalpic contributions of protein–ligand interactions.¹⁹
15
16

17
18 **Relationship of Binding Kinetics and Clinical Pharmacokinetics of Linagliptin.** The
19
20 gliptins described in this study are relatively similar with respect to translating their
21
22 pharmacodynamic effects into improvements in clinical efficacy.^{40, 41} Because DPP-4 activity is
23
24 inhibited by more than 80% over 24 h by most gliptins, they are administered as once-daily
25
26 drugs. An exception is vildagliptin, which is administered twice daily because of its relatively
27
28 short half-life.
29
30

31
32 The outstanding compound in the gliptin class is linagliptin because of its unique
33
34 nonlinear pharmacokinetics and mainly nonrenal elimination ($\leq 7\%$ excreted renally).⁴² The DPP-
35
36 4 protein exists in its major form as a membrane-bound protein expressed in nearly all tissues
37
38 with pronounced expression in kidney and liver; it also exists in soluble form in plasma. At very
39
40 low concentrations (e.g., < 1 nM), 99% of linagliptin is bound to circulating DPP-4 protein in
41
42 plasma and elimination is low. At higher concentrations (e.g., > 100 nM), the DPP-4 protein is
43
44 saturated and the proportion of protein binding decreases to 70–80%.⁴³ This results in an
45
46 increase in the free fraction of linagliptin and also its volume of distribution and clearance. From
47
48 those experiments, the dissociation constant of radiolabeled linagliptin to DPP-4 was
49
50 determined to be in the high affinity range of 10^{-10} M,⁴³ consistent with the biochemical activity
51
52 and biophysical data described above. Moreover, several studies have shown that the
53
54 concentration-dependent binding and biphasic pharmacokinetic behavior of linagliptin is totally
55
56
57
58
59
60

1
2
3 abolished in DPP-4-deficient rats or DPP-4 knockout mice,^{43, 44} indicating that a mechanism of
4 target-mediated drug deposition dominates the pharmacokinetics of linagliptin.
5
6

7
8 An additional consequence of this unique property of linagliptin may be more relevant
9 from a patient's perspective. With high levels of protein binding at clinically relevant linagliptin
10 concentrations, a low level of unbound drug is available for renal filtration. For linagliptin, the
11 renal excretion at its therapeutic dose is <7%. In contrast, other DPP-4 inhibitors are eliminated
12 primarily via the kidney. Evidence from DPP-4 knockout animals demonstrates this hypothesis,
13 as renal clearance of linagliptin (0.01 mg/kg, i.v. dosing) increases from 2.7% in wild-type mice
14 to 24.2% in the respective knockout mice.⁴³ As patients with type 2 diabetes often have impaired
15 renal function, dose adjustment of renally cleared drugs is indicated because of the potential for
16 drug accumulation and safety reasons. Of those gliptins currently marketed worldwide,
17 linagliptin is, so far, the only drug which does not require dose adjustment in all stages of renal
18 insufficiency.⁴⁵ Tenzeligliptin also does not require dose adjustment because the drug and its
19 main metabolite are eliminated via hepatic routes; renal elimination accounts for up to 20%.⁴⁶
20
21
22
23
24
25
26
27
28
29
30
31
32

33 All DPP-4 inhibitors have relatively low target dissociation rates. However, only linagliptin
34 exhibits a fast on-rate and an extraordinarily slow off-rate leading to a residence time of
35 approximately 5.5 h. The compound has affinity in the single-digit picomolar range and is
36 therefore orders of magnitude lower than DPP-4 protein concentrations in plasma and tissues.
37 Consequently, the drug undergoes continuous rebinding events which lead to the observed
38 phenomenon of target-mediated drug deposition in plasma and tissues, has a terminal
39 pharmacokinetic half-life of approximately 100 h as determined from clinical data,⁴⁷ and has a
40 high compound efficacy at very low therapeutic dose because of a high target occupancy at
41 stoichiometric concentrations. The additional rapid elimination of free drug leads to low systemic
42 exposure and a low rate of renal clearance.
43
44
45
46
47
48
49
50
51
52
53
54
55
56

57 **CONCLUSIONS**

58
59
60

1
2
3 In this study, DPP-4 inhibitors currently approved for the treatment of type 2 diabetes were
4 investigated, namely sitagliptin, vildagliptin, saxagliptin, linagliptin, alogliptin, and teneligliptin, as
5 well as a congeneric series of linagliptin precursors. SPR and ITC methods were used to
6 evaluate binding kinetics (k_{on} , k_{off} , K_D) and thermodynamics (ΔH , ΔS), and structural information
7 on ligand–DPP-4 complexes was used to discuss and interpret the biophysical data in the
8 context of three-dimensional structures.
9

10
11
12
13
14
15
16 The gliptins bind to DPP-4 in a rapid association regime (10^5 to 10^7 $M^{-1} s^{-1}$). This is
17 because of a Coulomb attraction between the negatively charged Glu-dyad within the DPP-4
18 active site and the positive charge on the ammonium moieties of the ligands. The fact that
19 primary amines, which have a larger charge build-up, associate faster than secondary amines
20 demonstrates that localized surface charges on both ligand and receptor contribute to binding
21 velocity. The slow dissociation of some gliptins (10^{-4} to 10^{-5} s^{-1}) is a result of two types of kinetic
22 barriers: the breaking of the covalent bond of the cyanopyrrolidines (saxagliptin and vildagliptin)
23 with the associated enlarged activation barrier for dissociation, or the dissolution of strong polar
24 and extensive hydrophobic interactions (linagliptin and teneligliptin). Finally, pairs of DPP-4
25 inhibitors with similar modes of binding and similar protein-induced conformational changes
26 show dissimilar binding kinetics. Therefore, in this scenario and in contrast to other reports,
27 conformational change has no dominant role in determining binding kinetics.
28
29
30
31
32
33
34
35
36
37
38
39
40
41

42 The series of congeneric linagliptin precursors also rapidly associate. The decrease in
43 k_{off} during compound progression correlates with binding affinity. The improvements in off-rates
44 were achieved through moieties that either form enhanced hydrogen bonding interactions or
45 cover larger hydrophobic surface areas.
46
47
48
49
50

51 All DPP-4 inhibitors exhibit a dominant enthalpic contribution to the free energy of
52 binding. This does not change during LO. The increase in binding affinity is fully reflected by
53 increasing binding enthalpy. Finally, the significant increase in lipophilicity does not influence
54 entropic effects but increases enthalpic contributions.
55
56
57
58
59
60

1
2
3 Using biophysical and biochemical methods, we have shown that linagliptin has, by far,
4 the highest affinity for DPP-4 with a K_D of 0.0066 nM. This is approximately 45 times more
5 potent than saxagliptin, the second best compound within the gliptin class. Further, the
6 residence time is four times longer for linagliptin than for saxagliptin or vildagliptin. The
7 extremely high affinity of linagliptin for DPP-4, the fast association rates, and the fact that DPP-4
8 target concentrations are much greater than the K_D , strongly suggests that rebinding is the
9 dominant mechanism behind the prolongation of the pharmacokinetic terminal half-life of
10 linagliptin. Despite an increasing number of recent examples in the literature, the molecular
11 determinants of binding kinetics remain poorly understood.^{12, 21} With the biophysical data and
12 their interpretation given in this manuscript, we intend to improve current understanding of the
13 underlying phenomena.
14
15
16
17
18
19
20
21
22
23
24
25
26
27
28

29 **EXPERIMENTAL SECTION**

31 **Materials.** Teneligliptin hydrobromide was purchased from BOC Sciences (Creative
32 Dynamics Inc., NY, USA) and had a stated purity of >98%. All other DPP-4 inhibitors were
33 synthesized in-house at Boehringer Ingelheim Pharma GmbH & Co. KG, Biberach, Germany
34 and had a general purity >95 % as determined by high performance liquid chromatography
35 and proton nuclear magnetic resonance (¹H-NMR). Recombinant human DPP-4 enzyme (aa 39-
36 766) was purchased from Proteros Biostructures GmbH (Munich, Germany).
37
38
39
40
41
42
43
44
45

46 **Inhibition of DPP-4 Activity from Human Blood or Recombinant Enzyme.**

47 Compounds were dissolved in DMSO (final concentration 0.1%), and inhibition of human
48 recombinant DPP-4 was assayed in black 96-well plates in assay buffer (100 mM Tris, 100 mM
49 NaCl, adjusted to pH 7.8 with HCl or NaOH) in the presence of 80 μ M substrate (H-Ala-Pro-7-
50 amido-4-trifluoromethylcoumarin [AlaPro-AFC]; from Bachem AG, Bubendorf, Switzerland) at
51 room temperature for 1 h. The final volume was 100 μ L and the final protein concentration was
52
53
54
55
56
57
58
59
60

1
2
3 10 ng/well corresponding to 1.2 nM. Fluorescence was detected using a Wallac Victor™ 1420
4
5 Multilabel Counter (PerkinElmer, Rodgau, Germany), at an excitation wavelength of 405 nm and
6
7 an emission wavelength of 535 nm. Human plasma was obtained from healthy male and female
8
9 individuals and collected in heparin-coated tubes (Sarstadt AG & Co, Nümbrecht, Germany);
10
11 DPP-4 activity was assayed as described above.
12
13

14
15
16 **Surface Plasmon Resonance Experiments.** DPP-4 was immobilized onto a CM5 chip
17
18 (GE Healthcare Bio-Sciences AB, Uppsala, Sweden) by amine coupling in 10 mM Na acetate at
19
20 pH 5.5. Binding studies were performed using a Biacore T200 instrument (GE Healthcare) at
21
22 25 °C in 20 mM Tris pH 7.3, 150 mM NaCl, 0.05% Tween 20, and 1% DMSO at a flow rate of 30
23
24 $\mu\text{L}/\text{min}$.
25
26

27
28 The interaction analyses were performed in the single-cycle kinetic mode using 120 s
29
30 association time and 7200 s dissociation time at the following DPP-4 inhibitor concentrations:
31
32 linagliptin 0.24, 0.74, 2.2, 6.6, and 20 nM; vildagliptin and saxagliptin 0.8, 4, 20, 100, and 500
33
34 nM; teneligliptin 0.16, 0.8, 4, 20, and 100 nM.
35

36
37 Alogliptin and sitagliptin were analyzed in the multi-cycle kinetic analysis mode using
38
39 120 s association time and 300 s (or 1800 s) dissociation time at analyte concentrations of 1.56,
40
41 3.1, 6.25, 12.5, 25, 50, and 100 nM. Kinetic parameters were analyzed using the Biacore T200
42
43 Evaluation Software 2.0 with the implemented 1:1 binding model.
44
45

46
47 **Isothermal Titration Calorimetry Analysis.** Experiments using isothermal titration
48
49 calorimetry were conducted on a MicroCal iTC200 instrument with DPP-4 that had been passed
50
51 through a PD-10 desalting column (GE Healthcare) equilibrated with 20 mM Tris pH 7.3 and 150
52
53 mM NaCl. Complete saturation of 5 μM DPP-4 inhibitor was typically achieved by injecting 18 \times
54
55 2 μL aliquots of 40 μM DPP-4 at 25 °C. Values obtained by reverse titration experiments were in
56
57 good agreement.
58
59
60

1
2
3 The thermodynamic binding parameters were extracted by nonlinear regression analysis
4 of the binding isotherms (MicroCal Origin software, version 7.0). A single-site binding model was
5 applied yielding the binding enthalpy (ΔH), stoichiometry (n), entropy (ΔS), and association
6 constant (K_a).
7
8
9

10
11 To ensure that the observed binding enthalpy was not affected by net proton release or
12 uptake upon ligand binding, control titrations in phosphate buffer were performed. The observed
13 ΔH from the titration experiments were plotted against $\Delta H_{\text{ionization}}$ of the two buffers. The slope of
14 the line (which gives the number of protons released by the buffers) does not indicate proton
15 release or uptake.
16
17
18
19
20
21
22

23 It should be noted that because of the high affinity of tested ligands, the values for the
24 association constant K_a may be prone to error. Therefore, a competition ITC experiment was
25 conducted for linagliptin, the most potent compound studied, in the presence of compound **1**.
26 These data were used to validate the thermodynamic parameters derived from direct titration
27 experiments (supporting information, see Figure S2).
28
29
30
31
32
33
34
35

36 ASSOCIATED CONTENT

37 Supporting Information

38
39 Supplementary data, including figures and tables, are presented for IC_{50} values of approved
40 DPP-4 inhibitors on human recombinant DPP-4 and plasma-derived DPP-4, kinetic on-off rate
41 plot of different DPP-4 inhibitors, isothermal titration of linagliptin in the presence of a
42 competition ligand, isothermal titration calorimetry of DPP-4 inhibitors, isothermal titration
43 calorimetry of linagliptin precursors, measured pKa and lipophilicity data (logD) for tested
44 compounds, crystal structure of compound **4** in porcine DPP-4, crystallographic data collection
45 and refinement statistics.
46
47
48
49
50
51
52
53
54
55
56
57
58
59
60

AUTHOR INFORMATION**Corresponding Author**

*Email: herbert.nar@boehringer-ingenelheim.com. Phone: +49 (0)7351 54 2888. Fax : +49 (0)7351 54 2165.

AUTHOR CONTRIBUTIONS

G.S. conceived the experimental design, analyzed the data and wrote the manuscript; T.K. contributed to research design and helped to prepare the manuscript; Y.H. carried out experiments; R.A.B. contributed to research design; H.N. contributed to research design, analyzed the data and wrote the manuscript.

CONFLICTS OF INTEREST

All authors are employees of Boehringer Ingelheim.

ACKNOWLEDGMENTS

This work was supported by Boehringer Ingelheim. The authors were fully responsible for all content and editorial decisions, were involved at all stages of manuscript development, and have approved the final version. We thank Dr Silke Retlich for helpful discussion regarding the pharmacokinetic aspects in the manuscript, Dr. Matthias Eckhardt for synthesis of Linagliptin and the precursors, and Dr. Michael Blaesse, Proteros Biostructures, for determining the initial co-structure of compound **4** with porcine DPP-4. Editorial assistance, supported by Boehringer Ingelheim, was provided by Paul MacCallum, PhD of Envision Scientific Solutions during the preparation of this manuscript.

ABBREVIATIONS USED

DPP-4, dipeptidyl peptidase-4

1
2
3 GIP, glucose-dependent insulinotropic peptide
4

5 GLP-1, glucagon-like peptide-1
6

7 IC₅₀, half maximal inhibitory concentration
8

9 ITC, isothermal titration calorimetry
10

11 LO, lead optimization
12

13 SPR, surface plasmon resonance
14

15 T, residence time, reciprocal of k_{off}
16
17
18
19
20
21
22
23
24
25
26
27
28
29
30
31
32
33
34
35
36
37
38
39
40
41
42
43
44
45
46
47
48
49
50
51
52
53
54
55
56
57
58
59
60

REFERENCES

1. Kieffer, T. J.; McIntosh, C. H.; Pederson, R. A. Degradation of glucose-dependent insulinotropic polypeptide and truncated glucagon-like peptide 1 in vitro and in vivo by dipeptidyl peptidase IV. *Endocrinology* **1995**, *136*, 3585–3596.
2. Meier, J. J.; Nauck, M. A.; Schmidt, W. E.; Gallwitz, B. Gastric inhibitory polypeptide: the neglected incretin revisited. *Regul. Pept.* **2002**, *107*, 1–13.
3. Egan, J. M.; Bulotta, A.; Hui, H.; Perfetti, R. GLP-1 receptor agonists are growth and differentiation factors for pancreatic islet beta cells. *Diabetes Metab. Res. Rev.* **2003**, *19*, 115–123.
4. Murphy, K. G.; Dhillo, W. S.; Bloom, S. R. Gut peptides in the regulation of food intake and energy homeostasis. *Endocr. Rev.* **2006**, *27*, 719–727.
5. McIntosh, C. H. Dipeptidyl peptidase IV inhibitors and diabetes therapy. *Front. Biosci.* **2008**, *13*, 1753–1773.
6. Rasmussen, H. B.; Branner, S.; Wiberg, F. C.; Wagtman, N. Crystal structure of human dipeptidyl peptidase IV/CD26 in complex with a substrate analog. *Nat. Struct. Biol.* **2003**, *10*, 19–25.
7. Golightly, L. K.; Drayna, C. C.; McDermott, M. T. Comparative clinical pharmacokinetics of dipeptidyl peptidase-4 inhibitors. *Clin. Pharmacokinet.* **2012**, *51*, 501–514.
8. Liu, Y.; Hu, Y.; Liu, T. Recent advances in non-peptidomimetic dipeptidyl peptidase 4 inhibitors: medicinal chemistry and preclinical aspects. *Curr. Med. Chem.* **2012**, *19*, 3982–3999.
9. Nabeno, M.; Akahoshi, F.; Kishida, H.; Miyaguchi, I.; Tanaka, Y.; Ishii, S.; Kadowaki, T. A comparative study of the binding modes of recently launched dipeptidyl peptidase IV inhibitors in the active site. *Biochem. Biophys. Res. Commun.* **2013**, *434*, 191–196.
10. Yoshida, T.; Akahoshi, F.; Sakashita, H.; Kitajima, H.; Nakamura, M.; Sonda, S.; Takeuchi, M.; Tanaka, Y.; Ueda, N.; Sekiguchi, S.; Ishige, T.; Shima, K.; Nabeno, M.; Abe, Y.;

1
2
3 Anabuki, J.; Soejima, A.; Yoshida, K.; Takashina, Y.; Ishii, S.; Kiuchi, S.; Fukuda, S.;
4
5 Tsutsumiuchi, R.; Kosaka, K.; Murozono, T.; Nakamaru, Y.; Utsumi, H.; Masutomi, N.; Kishida,
6
7 H.; Miyaguchi, I.; Hayashi, Y. Discovery and preclinical profile of teneligliptin (3-[(2S,4S)-4-[4-(3-
8
9 methyl-1-phenyl-1H-pyrazol-5-yl)piperazin-1-yl]pyrrolidin-2-yl carbonyl]thiazolidine): a highly
10
11 potent, selective, long-lasting and orally active dipeptidyl peptidase IV inhibitor for the treatment
12
13 of type 2 diabetes. *Bioorg. Med. Chem.* **2012**, *20*, 5705–5719.

14
15
16 11. Eckhardt, M.; Langkopf, E.; Mark, M.; Tadayyon, M.; Thomas, L.; Nar, H.; Pfrengle, W.;
17
18 Guth, B.; Lotz, R.; Sieger, P.; Fuchs, H.; Himmelsbach, F. 8-(3-(R)-aminopiperidin-1-yl)-7-but-2-
19
20 ynyl-3-methyl-1-(4-methyl-quinazolin-2-ylmethyl)-3,7-dihydropurine-2,6-dione (BI 1356), a
21
22 highly potent, selective, long-acting, and orally bioavailable DPP-4 inhibitor for the treatment of
23
24 type 2 diabetes. *J. Med. Chem.* **2007**, *50*, 6450–6453.

25
26
27 12. Cusack, K. P.; Wang, Y.; Hoemann, M. Z.; Marjanovic, J.; Heym, R. G.; Vasudevan, A.
28
29 Design strategies to address kinetics of drug binding and residence time. *Bioorg. Med. Chem.*
30
31 *Lett.* **2015**, *25*, 2019–2027.

32
33
34 13. Andersson, K.; Karlsson, R.; Lofas, S.; Franklin, G.; Hamalainen, M. D. Label-free kinetic
35
36 binding data as a decisive element in drug discovery. *Expert Opin. Drug Discovery* **2006**, *1*,
37
38 439–446.

39
40
41 14. Freire, E. Do enthalpy and entropy distinguish first in class from best in class? *Drug*
42
43 *Discovery Today* **2008**, *13*, 869–874.

44
45
46 15. Ladbury, J. E.; Klebe, G.; Freire, E. Adding calorimetric data to decision making in lead
47
48 discovery: a hot tip. *Nat. Rev. Drug Discovery* **2010**, *9*, 23–27.

49
50
51 16. Nunez, S.; Venhorst, J.; Kruse, C. G. Target-drug interactions: first principles and their
52
53 application to drug discovery. *Drug Discovery Today* **2012**, *17*, 10–22.

54
55
56 17. Klebe, G. Applying thermodynamic profiling in lead finding and optimization. *Nat. Rev.*
57
58 *Drug Discovery* **2015**, *14*, 95–110.
59
60

- 1
2
3 18. Liu, Y.; Hu, Y. Novel DPP-4 inhibitors against diabetes. *Future Med. Chem.* **2014**, *6*,
4 793–808.
5
6
7 19. Tummino, P. J.; Copeland, R. A. Residence time of receptor-ligand complexes and its
8 effect on biological function. *Biochemistry (Mosc.)* **2008**, *47*, 5481–5492.
9
10
11 20. Thomas, L.; Eckhardt, M.; Langkopf, E.; Tadayyon, M.; Himmelsbach, F.; Mark, M. (R)-
12 8-(3-amino-piperidin-1-yl)-7-but-2-ynyl-3-methyl-1-(4-methyl-quinazolin-2-ylm ethyl)-3,7-dihydro-
13 purine-2,6-dione (BI 1356), a novel xanthine-based dipeptidyl peptidase 4 inhibitor, has a
14 superior potency and longer duration of action compared with other dipeptidyl peptidase-4
15 inhibitors. *J. Pharmacol. Exp. Ther.* **2008**, *325*, 175–182.
16
17
18 21. Pan, A. C.; Borhani, D. W.; Dror, R. O.; Shaw, D. E. Molecular determinants of drug-
19 receptor binding kinetics. *Drug Discovery Today* **2013**, *18*, 667–673.
20
21
22 22. Wang, A.; Dorso, C.; Kopcho, L.; Locke, G.; Langish, R.; Harstad, E.; Shipkova, P.;
23 Marcinkeviciene, J.; Hamann, L.; Kirby, M. S. Potency, selectivity and prolonged binding of
24 saxagliptin to DPP4: maintenance of DPP4 inhibition by saxagliptin in vitro and ex vivo when
25 compared to a rapidly-dissociating DPP4 inhibitor. *BMC Pharmacol.* **2012**, *12*, 2.
26
27
28 23. Metzler, W. J.; Yanchunas, J.; Weigelt, C.; Kish, K.; Klei, H. E.; Xie, D.; Zhang, Y.;
29 Corbett, M.; Tamura, J. K.; He, B.; Hamann, L. G.; Kirby, M. S.; Marcinkeviciene, J. Involvement
30 of DPP-IV catalytic residues in enzyme-saxagliptin complex formation. *Protein Sci.* **2008**, *17*,
31 240-250.
32
33
34 24. Schmidtke, P.; Luque, F. J.; Murray, J. B.; Barril, X. Shielded hydrogen bonds as
35 structural determinants of binding kinetics: application in drug design. *J. Am. Chem. Soc.* **2011**,
36 *133*, 18903–18910.
37
38
39 25. Copeland, R. A. Conformational adaptation in drug-target interactions and residence
40 time. *Future Med. Chem.* **2011**, *3*, 1491–1501.
41
42
43
44
45
46
47
48
49
50
51
52
53
54
55
56
57
58
59
60

- 1
2
3
4
5
6
7
8
9
10
11
12
13
14
15
16
17
18
19
20
21
22
23
24
25
26
27
28
29
30
31
32
33
34
35
36
37
38
39
40
41
42
43
44
45
46
47
48
49
50
51
52
53
54
55
56
57
58
59
60
26. Biela, A.; Nasief, N. N.; Betz, M.; Heine, A.; Hangauer, D.; Klebe, G. Dissecting the hydrophobic effect on the molecular level: the role of water, enthalpy, and entropy in ligand binding to thermolysin. *Angew. Chem. Int. Ed. Engl.* **2013**, *52*, 1822–1828.
27. Steuber, H.; Heine, A.; Klebe, G. Structural and thermodynamic study on aldose reductase: nitro-substituted inhibitors with strong enthalpic binding contribution. *J. Mol. Biol.* **2007**, *368*, 618–638.
28. Abel, R.; Young, T.; Farid, R.; Berne, B. J.; Friesner, R. A. Role of the active-site solvent in the thermodynamics of factor Xa ligand binding. *J. Am. Chem. Soc.* **2008**, *130*, 2817–2831.
29. Young, T.; Abel, R.; Kim, B.; Berne, B. J.; Friesner, R. A. Motifs for molecular recognition exploiting hydrophobic enclosure in protein-ligand binding. *Proc. Natl. Acad. Sci. U. S. A.* **2007**, *104*, 808–813.
30. Nguyen, C. N.; Cruz, A.; Gilson, M. K.; Kurtzman, T. Thermodynamics of Water in an Enzyme Active Site: Grid-Based Hydration Analysis of Coagulation Factor Xa. *J. Chem. Theory Comput.* **2014**, *10*, 2769–2780.
31. Nguyen, C. N.; Young, T. K.; Gilson, M. K. Grid inhomogeneous solvation theory: hydration structure and thermodynamics of the miniature receptor cucurbit[7]uril. *J. Chem. Phys.* **2012**, *137*, 044101.
32. Ruhmann, E.; Betz, M.; Fricke, M.; Heine, A.; Schafer, M.; Klebe, G. Thermodynamic signatures of fragment binding: Validation of direct versus displacement ITC titrations. *Biochim. Biophys. Acta* **2015**, *1850*, 647–656.
33. Schuck, P.; Zhao, H. The role of mass transport limitation and surface heterogeneity in the biophysical characterization of macromolecular binding processes by SPR biosensing. *Methods Mol. Biol.* **2010**, *627*, 15–54.
34. Copeland, R. A.; Pompliano, D. L.; Meek, T. D. Drug-target residence time and its implications for lead optimization. *Nat. Rev. Drug Discovery* **2006**, *5*, 730–739.

- 1
2
3 35. Ferenczy, G. G.; Keseru, G. M. Thermodynamics guided lead discovery and
4 optimization. *Drug Discovery Today* **2010**, *15*, 919–932.
5
6
7 36. Holdgate, G. A. Thermodynamics of binding interactions in the rational drug design
8 process. *Expert Opin. Drug Discovery* **2007**, *2*, 1103–1114.
9
10
11 37. Swinney, D. C. The role of binding kinetics in therapeutically useful drug action. *Curr.*
12 *Opin. Drug Discovery Dev.* **2009**, *12*, 31–39.
13
14
15 38. Englert, L.; Biela, A.; Zayed, M.; Heine, A.; Hangauer, D.; Klebe, G. Displacement of
16 disordered water molecules from hydrophobic pocket creates enthalpic signature: binding of
17 phosphoramidate to the S(1)'-pocket of thermolysin. *Biochim. Biophys. Acta* **2010**, *1800*, 1192–
18 1202.
19
20
21 39. Krimmer, S. G.; Betz, M.; Heine, A.; Klebe, G. Methyl, ethyl, propyl, butyl: futile but not
22 for water, as the correlation of structure and thermodynamic signature shows in a congeneric
23 series of thermolysin inhibitors. *ChemMedChem* **2014**, *9*, 833–846.
24
25
26 40. Scheen, A. J. A review of gliptins in 2011. *Expert Opin. Pharmacother.* **2012**, *13*, 81–99.
27
28
29 41. Scheen, A. J. A review of gliptins for 2014. *Expert Opin. Pharmacother.* **2015**, *16*, 43–62.
30
31
32 42. Graefe-Mody, U.; Retlich, S.; Friedrich, C. Clinical pharmacokinetics and
33 pharmacodynamics of linagliptin. *Clin. Pharmacokinet.* **2012**, *51*, 411–427.
34
35
36 43. Fuchs, H.; Tillement, J. P.; Urien, S.; Greischel, A.; Roth, W. Concentration-dependent
37 plasma protein binding of the novel dipeptidyl peptidase 4 inhibitor BI 1356 due to saturable
38 binding to its target in plasma of mice, rats and humans. *J. Pharm. Pharmacol.* **2009**, *61*, 55–62.
39
40
41 44. Retlich, S.; Withopf, B.; Greischel, A.; Staab, A.; Jaehde, U.; Fuchs, H. Binding to
42 dipeptidyl peptidase-4 determines the disposition of linagliptin (BI 1356)--investigations in DPP-
43 4 deficient and wildtype rats. *Biopharm. Drug Dispos.* **2009**, *30*, 422–436.
44
45
46 45. Graefe-Mody, U.; Friedrich, C.; Port, A.; Ring, A.; Retlich, S.; Heise, T.; Halabi, A.;
47 Woerle, H. J. Effect of renal impairment on the pharmacokinetics of the dipeptidyl peptidase-4
48 inhibitor linagliptin(*). *Diabetes Obes. Metab.* **2011**, *13*, 939–946.
49
50
51
52
53
54
55
56
57
58
59
60

- 1
2
3 46. Halabi, A.; Maatouk, H.; Siegler, K. E.; Faisst, N.; Lufft, V.; Klause, N. Pharmacokinetics
4 of teneligliptin in subjects with renal impairment. *Clin. Pharmacol. Drug Dev.* **2013**, *2*, 246–254.
5
6
7 47. Retlich, S.; Duval, V.; Graefe-Mody, U.; Jaehde, U.; Staab, A. Impact of target-mediated
8 drug disposition on Linagliptin pharmacokinetics and DPP-4 inhibition in type 2 diabetic patients.
9
10
11 *J. Clin. Pharmacol.* **2010**, *50*, 873–885.
12
13
14 48. Kim, D.; Wang, L.; Beconi, M.; Eiermann, G. J.; Fisher, M. H.; He, H.; Hickey, G. J.;
15
16 Kowalchick, J. E.; Leiting, B.; Lyons, K.; Marsilio, F.; McCann, M. E.; Patel, R. A.; Petrov, A.;
17
18 Scapin, G.; Patel, S. B.; Roy, R. S.; Wu, J. K.; Wyvratt, M. J.; Zhang, B. B.; Zhu, L.; Thornberry,
19
20 N. A.; Weber, A. E. (2R)-4-oxo-4-[3-(trifluoromethyl)-5,6-dihydro[1,2,4]triazolo[4,3-a]pyrazin-
21
22 7(8H)-yl]-1-(2,4,5-trifluorophenyl)butan-2-amine: a potent, orally active dipeptidyl peptidase IV
23
24 inhibitor for the treatment of type 2 diabetes. *J. Med. Chem.* **2005**, *48*, 141-151.
25
26
27 49. Zhang, Z.; Wallace, M. B.; Feng, J.; Stafford, J. A.; Skene, R. J.; Shi, L.; Lee, B.;
28
29 Aertgeerts, K.; Jennings, A.; Xu, R.; Kassel, D. B.; Kaldor, S. W.; Navre, M.; Webb, D. R.;
30
31 Gwaltney, S. L. Design and synthesis of pyrimidinone and pyrimidinedione inhibitors of
32
33 dipeptidyl peptidase IV. *J. Med. Chem.* **2011**, *54*, 510-524.
34
35
36
37
38
39
40
41
42
43
44
45
46
47
48
49
50
51
52
53
54
55
56
57
58
59
60

FIGURE LEGENDS

Figure 1. Co-structures of DPP-4 inhibitors bound within the DPP-4 active site.

DPP-4 inhibitors with a similar binding mode in X-ray structures are shown as overlaid pairs.

(a) DPP-4 active site with saxagliptin (3BJM²³, cyan) and vildagliptin (3W2T⁹, purple) bound; (b)

DPP-4 active site with sitagliptin (1X70⁴⁸, cyan) and teneligliptin (3VJK¹⁰, purple) bound; (c)

DPP-4 active site with linagliptin (2RGU¹¹, cyan) and alogliptin (3G0B⁴⁹, purple) bound. In each figure, a superposition of the structures of free (white carbon atoms) and ligand bound (yellow carbon atoms) enzyme shows protein structural changes upon ligand binding.

Key interaction residues are indicated in black; residues involved in structural rearrangements upon binding are indicated in red. Protein data bank (PDB) accession codes for the various X-ray structures are indicated in brackets above.

Figure 2. Binding kinetics of approved DPP-4 inhibitors studied with surface plasmon resonance.

Sitagliptin and alogliptin were studied using multi-cycle binding kinetics, whereas the other DPP-4 inhibitors were studied using single-cycle kinetics. Teneligliptin is shown and fitted as a single concentration measurement. The x-axis in the sensorgrams represents the time in seconds; the y-axis represents the signal in responsive units. The colored lines represent experimental data and the black line represents the fitted curve. The sensorgrams show representative examples.

The kinetic data were mean values from two independent measurements with calculated standard deviation. Residence time τ was calculated as the reciprocal of the mean k_{off} value ($\tau = 1/k_{\text{off}}$).

Figure 3. Thermodynamic profiles of the gliptins binding to DPP-4 based on isothermal titration calorimetry experiments.

1
2
3 The experimentally derived parameters include the Gibbs free energy of binding (ΔG , blue bar),
4 the enthalpy change (ΔH , green bar), and the temperature-dependent entropy change ($-T\Delta S$,
5 red bar). 40 μM of DPP-4 was titrated into 5 μM of DPP-4 inhibitor. Data are mean values from
6
7
8 at least two titrations with calculated standard deviation.
9
10

11
12
13
14 **Figure 4.** Chemical structures of the initial hit compound **1** from high-throughput screening (a),
15 two precursors of linagliptin compounds **2** and **3** (b and c) and linagliptin (d). The numbers in red
16 (Fig. 4a) indicate the position of the substituent in the xanthine core.
17
18
19

20
21
22
23 **Figure 5.** Binding kinetics of linagliptin precursor molecules studied with surface plasmon
24 resonance.
25

26
27 Compounds **1** and **2** were studied by multi-cycle binding kinetics, whereas compound **3** and
28 linagliptin were studied by single-cycle kinetics. The sensorgrams show representative
29 examples. The x-axis in the sensorgrams represents the time in seconds; the y-axis represents
30 the signal in responsive units. The colored lines represent experimental data and the black line
31 represents the fitted curve. The kinetic data were mean values from two independent
32 measurements with calculated standard deviation.
33
34
35
36
37
38
39
40
41

42
43 **Figure 6.** Thermodynamic profile of linagliptin and its precursors binding to DPP-4 based on
44 isothermal titration calorimetry experiments. The experimentally derived parameters include the
45 Gibbs free energy of binding (ΔG , blue bar), the enthalpy change (ΔH , green bar), and the
46 temperature dependent entropy change ($-T\Delta S$, red bar). 40 μM of compound **1**, **2**, **3**, or
47 linagliptin were titrated into 5 μM DPP-4. Data are mean values from at least two titrations with
48
49
50
51
52
53
54
55
56
57
58
59
60

1
2
3 **Figure 7.** X-ray structures of linagliptin precursors in complex with DPP-4 in a surface
4 representation with calculated surface charges (Pymol).
5
6
7
8 (a) shows the initial HTS hit (2AJ8 compound **1**), (b) is the X-ray structure of a Br-derivative of
9 compound **2** (compound **4** – *structure submitted to PDB database/awaiting PDB accession*
10 *code*), (c) shows compound **3** modeled in the active site, and (d) is the X-ray structure of
11 linagliptin (2RGU). PDB accession codes of X-ray structures are indicated in brackets when
12 applicable.
13
14
15
16
17
18
19
20
21
22
23
24
25
26
27
28
29
30
31
32
33
34
35
36
37
38
39
40
41
42
43
44
45
46
47
48
49
50
51
52
53
54
55
56
57
58
59
60

FIGURES

Figure 1.

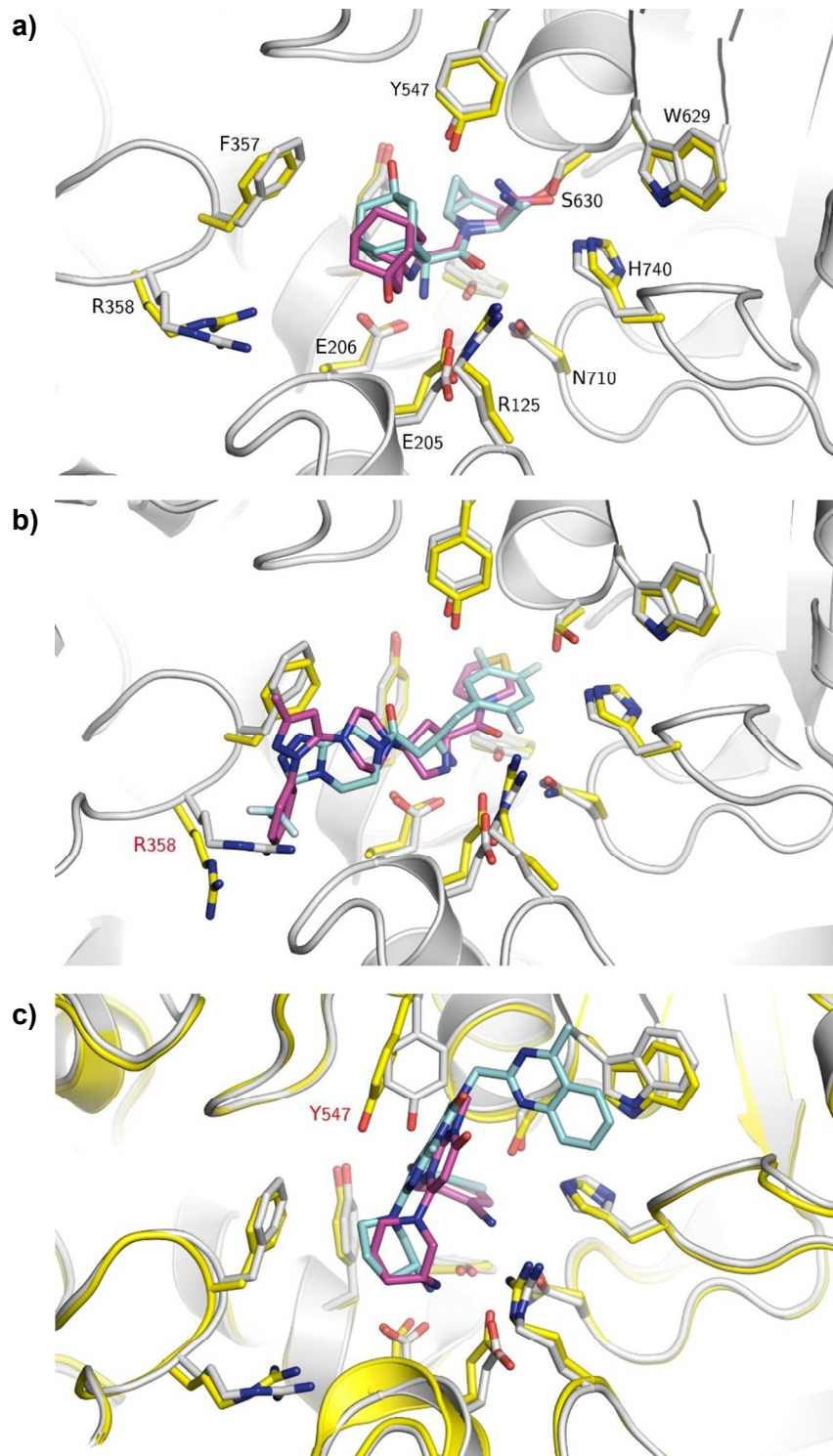


Figure 2.

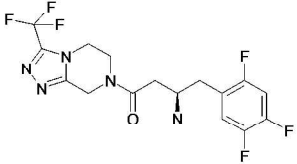
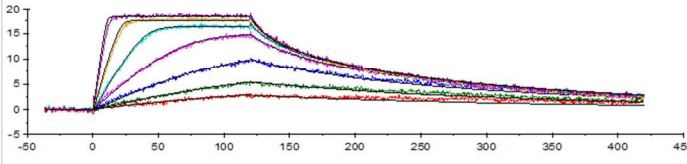
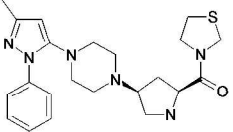
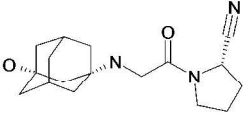
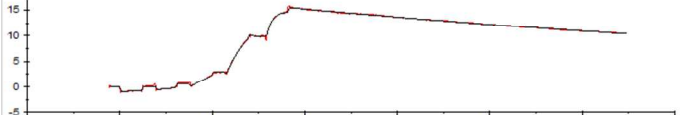
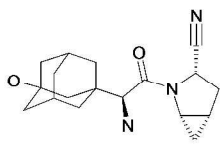
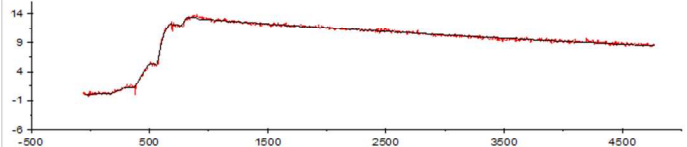
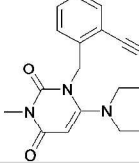
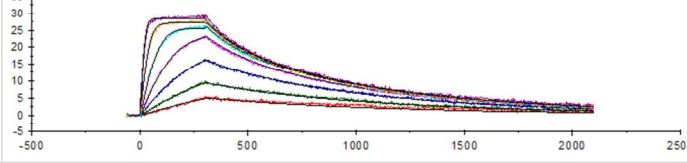
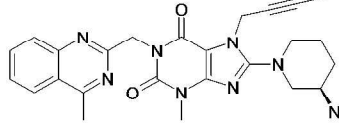
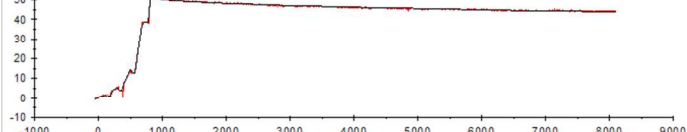
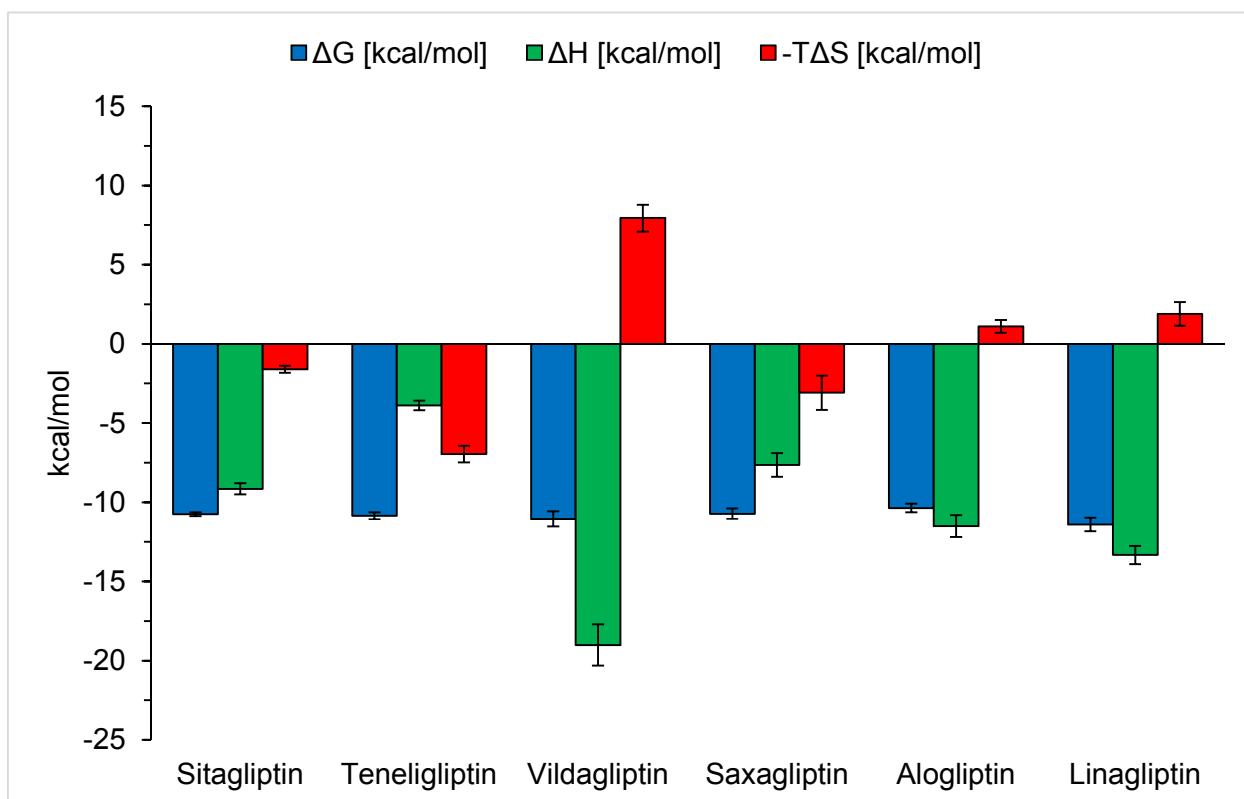
Compound Name	Chemical Structure	SPR Sensorgram	K_D [nM]	k_{on} [$M^{-1}s^{-1}$]	$k_{off} \times 10^{-4}$ [s^{-1}]	T [min]
Sitagliptin			5.3 ± 1.4	$(1.5 \pm 0.9) \times 10^7$	630 ± 260	0.26
Teneligliptin			0.41 ± 0.015	$(6.5 \pm 0.4) \times 10^5$	2.6 ± 0.2	64
Vildagliptin			2.4 ± 0.7	$(7.1 \pm 0.07) \times 10^4$	1.7 ± 0.5	98
Saxagliptin			0.3 ± 0.1	$(9.2 \pm 7.4) \times 10^5$	2.0 ± 1.0	83
Alogliptin			2.4 ± 0.1	$(1.3 \pm 0.1) \times 10^6$	31 ± 5	5.4
Linagliptin			0.0066 ± 0.00034	$(7.6 \pm 1.8) \times 10^6$	0.51 ± 0.14	327

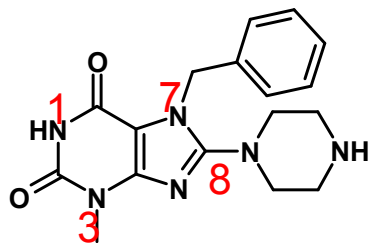
Figure 3.



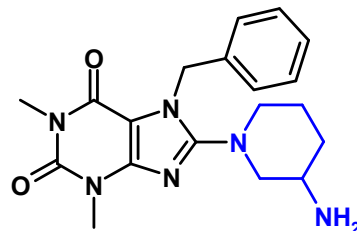
Compound	ΔG [kcal/mol]	ΔH [kcal/mol]	$-T\Delta S$ [kcal/mol]	K_D [nM]
Sitagliptin	-10.74 ± 0.12	-9.14 ± 0.35	-1.61 ± 0.23	13.5 ± 2.7
Teneligliptin	-10.84 ± 0.22	-3.89 ± 0.31	-6.95 ± 0.52	11.9 ± 4.2
Vildagliptin	-11.05 ± 0.48	-19.00 ± 1.30	7.94 ± 0.85	10.7 ± 7.2
Saxagliptin	-10.72 ± 0.33	-7.64 ± 0.75	-3.09 ± 1.08	15.9 ± 7.9
Alogliptin	-10.35 ± 0.27	-11.50 ± 0.70	1.11 ± 0.41	28.5 ± 12.3
Linagliptin	-11.40 ± 0.44	-13.33 ± 0.57	1.90 ± 0.75	5.3 ± 3.6

Figure 4.

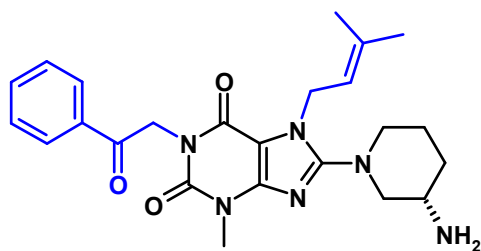
a)

 $IC_{50}: 3900 \text{ nM}$

b)

 $IC_{50}: 82$

c)

 $IC_{50}: 5 \text{ nM}$

d)

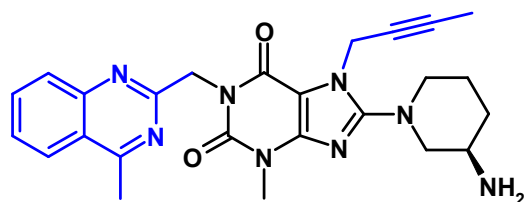
 $IC_{50}: 1 \text{ nM}$

Figure 5.

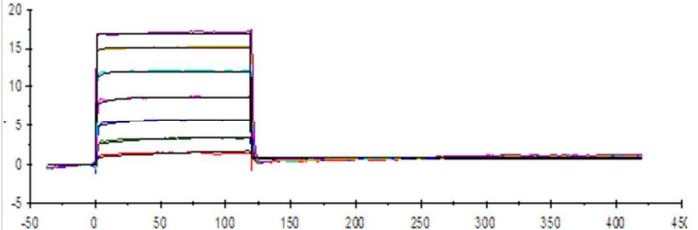
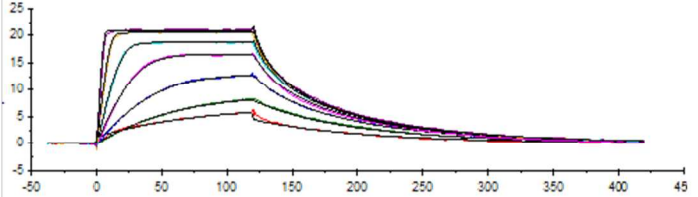
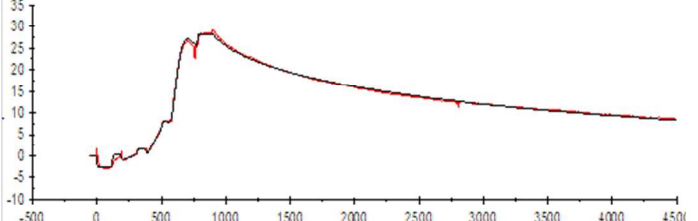
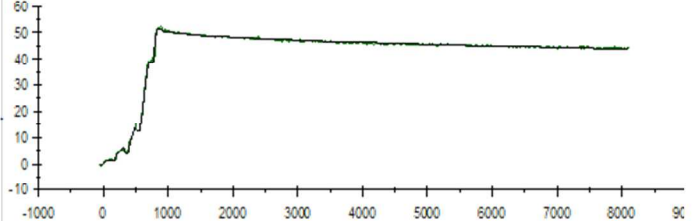
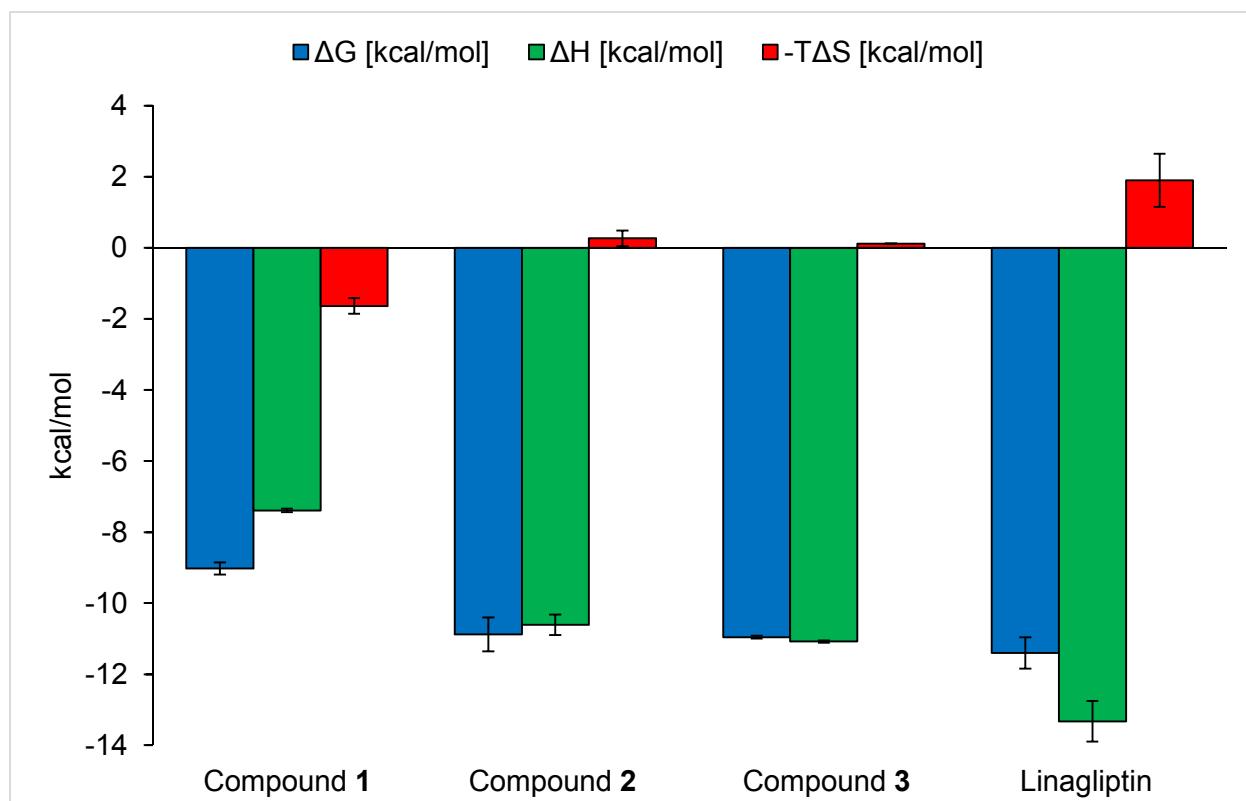
Compound	SPR Sensorgram	K_D [nM]	$k_{on} \times 10^6$ [$M^{-1}s^{-1}$]	$k_{off} \times 10^{-4}$ [s^{-1}]
1		806 ± 36		
2		13.2 ± 0.5	4.8 ± 1.4	640 ± 140
3		0.42 ± 0.08	4.4 ± 0.3	18.6 ± 4.6
Linagliptin		0.0066 ± 0.00034	7.6 ± 1.8	0.51 ± 0.14

Figure 6.



Compound	ΔG [kcal/mol]	ΔH [kcal/mol]	$-T\Delta S$ [kcal/mol]	K_D [nM]
Compound 1	-9.03 ± 0.17	-7.39 ± 0.05	-1.64 ± 0.22	246 ± 67
Compound 2	-10.88 ± 0.48	-10.61 ± 0.29	0.27 ± 0.22	18.6 ± 8.3
Compound 3	-10.96 ± 0.04	-11.08 ± 0.03	0.12 ± 0.01	9.2 ± 0.6
Linagliptin	-11.40 ± 0.44	-13.33 ± 0.57	1.90 ± 0.75	5.6 ± 3.6

Figure 7.

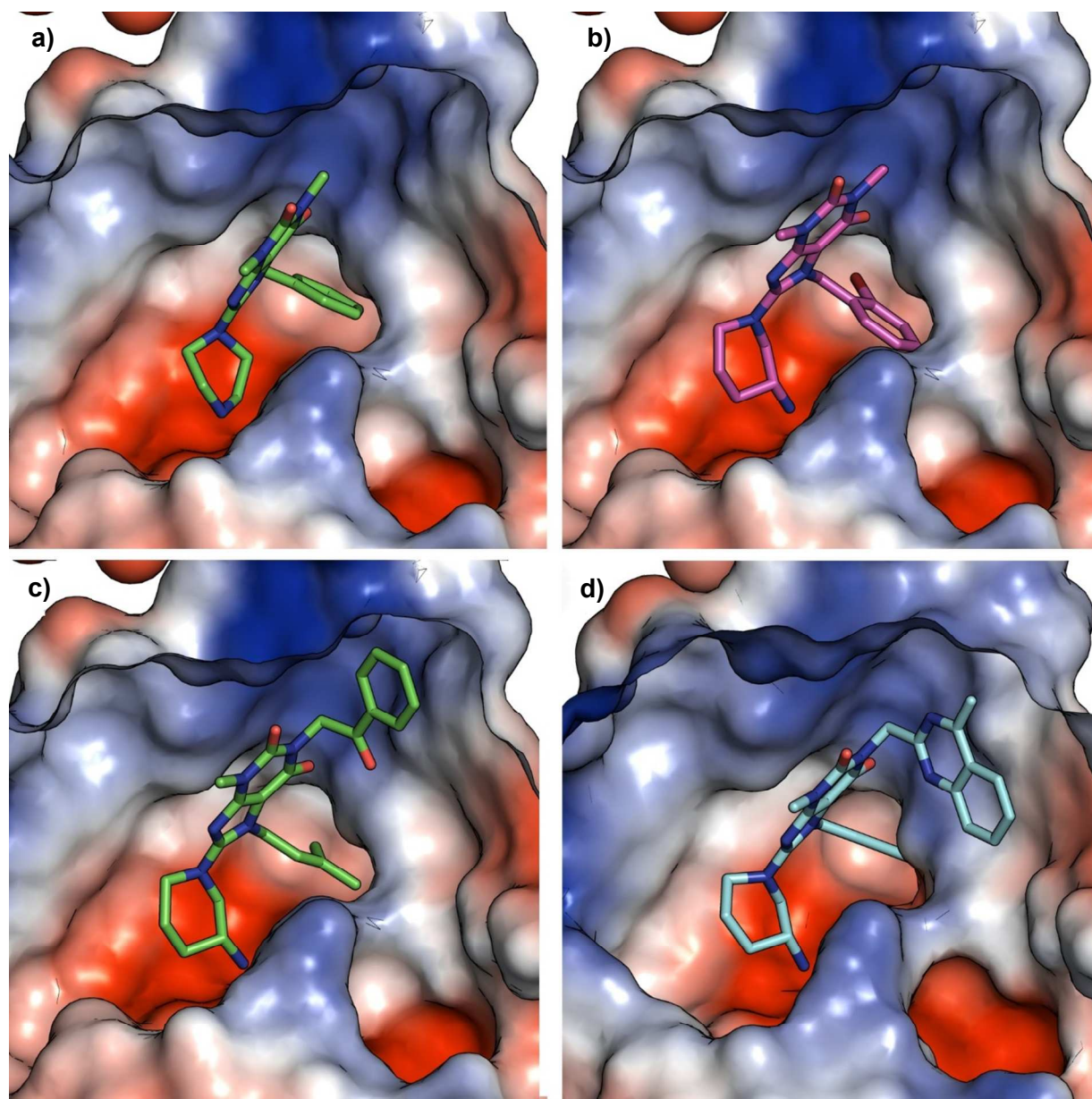


TABLE OF CONTENTS GRAPHIC

